



# NJC

## Quantitative and Highly Selective Sensing of Sodium Houttuynonate via Long-aliphatic chains Hydrophobic Assemble and Aggregation-Induced Emission

Journal:	<i>New Journal of Chemistry</i>
Manuscript ID	NJ-ART-04-2015-001036.R2
Article Type:	Paper
Date Submitted by the Author:	29-Aug-2015
Complete List of Authors:	<p>yang, yunxu; University of Science and Technology Beijing, Department of Chemistry and Chemical Engineering, School of Chemistry and Biological Engineering</p> <p>yu, feifei; University of Science and Technology Beijing, Department of Chemistry and Chemical Engineering, School of Chemistry and Biological Engineering</p> <p>Wang, Aizhi; University of Science and Technology Beijing, 1. Department of Chemistry and Chemical Engineering</p> <p>hu, biwei; University of Science and Technology Beijing, Department of Chemistry and Chemical Engineering, School of Chemistry and Biological Engineering</p> <p>Luo, Xiaofei; 3. College of Chemistry and Molecular Engineering, Zhengzhou University,</p> <p>Sheng, Ruilong; 2. Key laboratory of Synthesis and Self-assembly of Organic Functional Materials, CAS. Shanghai Institute of Organic Chemistry,</p> <p>Dong, Yajun; University of Science and Technology Beijing, 1. Department of Chemistry and Chemical Engineering</p> <p>fan, weiping; University of Science and Technology Beijing, Department of Chemistry and Chemical Engineering, School of Chemistry and Biological Engineering</p>

# Quantitative and Highly Selective Sensing of Sodium Houttuayfonate via Long-aliphatic chains Hydrophobic Assemble and Aggregation-Induced Emission

*Feifei Yu<sup>1</sup>, Yunxu Yang<sup>1,\*</sup>, Aizhi Wang<sup>1</sup>, Biwei Hu<sup>1</sup>, Xiaofei Luo<sup>3</sup>, Ruilong Sheng<sup>2,\*</sup>, Yajun Dong<sup>1</sup>,*

*Weiping Fan<sup>1</sup>*

1. Department of Chemistry and Chemical Engineering, University of Science and Technology

Beijing, Beijing 100083, China.

2. Key laboratory of Synthesis and Self-assembly of Organic Functional Materials, CAS.

Shanghai Institute of Organic Chemistry, Shanghai 200032, China.

3. College of Chemistry and Molecular Engineering, Zhengzhou University, Zhengzhou,  
Henan, 450001, China

## Corresponding Authors

\*Yunxu Yang, E-mail: [yxyang@ustb.edu.cn](mailto:yxyang@ustb.edu.cn) Fax: (+86)-10-6233-3871

\*Ruilong Sheng, E-mail: [rayleigh121@aliyun.com](mailto:rayleigh121@aliyun.com)

**Abstract**

A new  $\alpha$ -cyanostilbene derivative, **CDB-DMA12**, was designed and synthesized as a supramolecular chemosensor for the detection of Sodium Houttuynonate (**SH**) via aggregation-induced emission enhancement (AIEE), which could efficiently bind with SH, then induce obvious fluorescence enhancement and visible absorption red-shifting (by naked eyes). Accordingly, a linear relationship was found when plot the fluorescence intensity at 558 nm against SH concentration, with an estimated detection limit of 8.5  $\mu\text{M}$ . Interestingly, morphology changes from nanoparticle to sheet, scroll and tube-shaped aggregates were observed on **CDB-DMA12** after addition of SH. Moreover, **CDB-DMA12** showed high selectivity to SH among other sulfonyl containing species, attributed to the synergistic effect of its quaternary ammonium, the hydrogen binding of the active group sites and a twelve carbon containing long-aliphatic chain units. In addition, the results paved a new way for detection/recognition of amphiphilic natural products in aqueous solution with high sensitivity and selectivity. Besides, it provided a possible approach for preparation of new fluorescent micro/nano-scaled architectures through solution self-assembly of oppositely-charged amphiphiles.

**Key Words:** aggregation-induced emission, electrostatic interaction, self-assembly, fluorescence, Sodium Houttuynonate

## 1. Introduction

Houttuynin, one of the main active constituent in the volatile oil of the Asian plant *Houttuynia Cordata* Thunb, was firstly isolated by Kosuge in 1952.<sup>1</sup> Houttuynin is likely inactivated by oxidation or polymerization after extraction, so it was further reacted with sodium bisulfite to prepare Sodium Houttuynifonate (**SH**, decanoyl acetaldehyde sodium sulfite), a more steady form with similar pharmaceutical activity.<sup>2</sup> Clinically, **SH** has been employed as an antimicrobial medicine to effectively inhibit the growth of G<sup>+</sup>-bacteria such as *S. aureus*, *M. catarrhalis*, *B. influenzae*, and *S. pneumoniae* for many years.<sup>3-5</sup> Prior researches also disclosed that **SH** have some other pharmaceutical and biological functions such as immunological enhancement and lysozyme function modulating activities both *in vitro* and *in vivo*.<sup>6-9</sup> Therefore, the quantitative detection of **SH** has attracted much attention in recent years. Although many efforts for **SH** detection such as HPLC,<sup>10</sup> UPLC-MS,<sup>11</sup> etc., have been put into development and application, highly sensitive, selective and real-time analytical methods for **SH** detection is still rare and is of high demand.

As a rapid and convenient analytical approach, developing new fluorescent probes with the advantage of real-time analysis, easy manipulation, high selectivity and sensitivity for small organic molecular sensing/detecting have received considerable attention.<sup>12-16</sup> Recently, some chemosensors based on molecular aggregation induced emission enhancement (AIEE),<sup>17-19</sup> were developed and utilized as efficient fluorescent chemosensors for the detection of small organic

molecules and biomolecules.<sup>20-35</sup> Among these new AIE luminogens,  $\alpha$ -cyanostilbene derivative, a power optical sensing platform based on  $\pi$ -conjugated molecules comprising a cyanostilbene backbone with terminal functional groups offers a unique combination of high sensitivity and visual detection.<sup>36-41</sup> We have also constructed two  $\pi$ -conjugated cyanostilbene derivatives which possesses an unusual high emissive aggregation-induced emission (AIE) feature and could be used as the detection probe of  $\text{Hg}^{2+}$  or  $\text{Cu}^{2+}$ .<sup>40, 34</sup> Meanwhile, several kinds of water-stable and adaptive materials mainly based on the strategy of intermolecular electrostatic and hydrophobic interactions have been developed for bioanalysis, bioimaging and the fluorescent detection.<sup>42-51</sup>

Based on the above thinking, we designed and synthesized a series of quaternary ammonium salts of cyanostilbene derivatives (as shown in S1, Supporting Information). However, diversity characterizations of these derivatives showed no selectivity and sensitivity except a cyanostilbene derivate of **CDB-DMA12** which has a ‘turn-on’ response for **SH** via AIEE. Herein, we reported the new direct fluorometric ‘turn-on’ assay for **SH** by using **CDB-DMA12** via AIEE. The detecting rationale for this new fluorometric detection of **SH** is schematically illustrated in Scheme 1. **CDB-DMA12** with a positive ammonium group shows weak fluorescence in aqueous solution. But, in the presence of an amphiphilic compound of **SH** with a negatively charged group, aggregation would occur due to the intermolecular electrostatic and hydrophobic interactions; as a result the fluorescence of **CDB-DMA12** is switched on. The interaction/recognition between **CDB-DMA12** and **SH** was measured by fluorescence spectra and UV-vis absorption, and the aggregation/assembly of **CDB-DMA12/SH** in solution was

further investigated by dynamic light scattering (DLS) and transmission electron microscope (TEM) measurement. Moreover, the selectivity of **CDB-DMA12** to **SH** among other sulfonyl-containing species was also measured for the purposes of comparison, and the possible recognition and aggregation mechanisms between **CDB-DMA12** and **SH** was proposed and discussed. All of the results revealed that a fluorescence turn-on detection of **SH** in aqueous solution can be established with **CDB-DMA12**. To our best knowledge, up to now, successful examples for direct fluorescent detection of **SH** by using aggregation induced fluorescence change were rarely reported, thus, the development of convenient, high selective and sensitive chemosensors for **SH** detection/recognition was still a big challenge.

## 2. Experimental section

### 2.1 Materials and Apparatus

The sodium houthuyfonate (**SH**, reference material, 99.9%) was purchased from National Institutes for Food and Drug Control. phenylacetonitrile (98%), 4-Nitrobenzaldehyde (98%), 4-Nitrophenylacetonitrile (98%), 4-Hydroxybenzaldehyde (98%), 1,4-dibromobutane (98%) , N,N-dimethyldodecylamine (98%), **SDS** (99%), Benzaldehyde (99%), Propionaldehyde (99%), Sodium Bisulfite (98%) were purchased from *Alfa Aesar*. Other reagents were purchased from *Beijing Chemical Regent Co*. All the other chemicals obtained from commercial sources were analytical pure and used without further purification unless otherwise noted. Analytical TLC was

carried out on silica gel plates (HSGF254) *Yantai Chemical Industry Research Institute*) and compounds were visualized by UV-light and iodine.

$^1\text{H}$  NMR and  $^{13}\text{C}$  NMR spectra were recorded on Varian Gemini-400 (Bruker, 400 MHz) NMR spectrometer with tetramethylsilane as an internal standard. MALDI-TOF was recorded on Bruker Daltonics Inc. BIFLEX-III spectrometers. Electrospray ionization (ESI) mass spectra were collected on Bruker Daltonics Inc. APEX-II spectrometers. Electron impact (EI) mass spectroscopy was carried out on a Waters GCT Premier XE mass spectrometer. All UV-visible and fluorescence spectra in this work were recorded on Pgeneral TU-1901 and Hitachi F-4500 fluorescence spectrometers and at 25°C. Transmission Electron Microscope (TEM) was recorded on JEM-2010. Dynamic Light Scattering (DLS) were recorded on a Malvern Nano-ZS instrument. The water was purified by Millipore filtration system. Melting points were measured with RD-II melting point apparatus (*Tainjin Xintianguang Instrument Company*).

## 2.2 Synthesis

The synthetic routes and the synthetic details of the quaternary ammonium salts of  $\alpha$ -cyanostilbene derivatives **CDB1-5** were outlined and described in S2. While, **CDB-DMA12**, Model **1** and Model **2** were outlined in Scheme **2**, and the synthetic details were described below.

### Synthesis of (Z)-3-(4-hydroxyphenyl)-2-(4-nitrophenyl)acrylonitrile (**1**)

To a mixture of 4-hydroxybenzaldehyde (0.122 g, 0.001 mol) and 4-nitrobenzylcyanide (0.162g, 0.001mol) in EtOH (5 mL), piperidine (0.255 g, 0.003 mol) was added with dropwise and stirred at room temperature for 3 h, then cooled to 0°C. The precipitate was filtered

and recrystallized from THF/water/HCl first, and then purified by column chromatography (CH<sub>2</sub>Cl<sub>2</sub> : petroleum=1: 2 was used as eluent). A yellow solid was obtained (0.246 g, 92%). mp 231-233 °C IR(KBr):  $\nu$  3402, 2214, 1585, 1571, 1510, 1442, 1338, 1170, 852 cm<sup>-1</sup>; <sup>1</sup>H NMR (400 MHz, DMSO-d<sub>6</sub>):  $\delta$  10.46 (s, 1H), 8.32 (d,  $J$ =8.4 Hz, 2H), 8.16 (s, 1H), 7.99-7.92 (m, 4H), 6.94 (d,  $J$ =8.4Hz, 2H); <sup>13</sup>C NMR (DMSO-d<sub>6</sub>)  $\delta$  (ppm): 161.35, 147.26, 146.81, 141.22, 132.51, 126.94, 124.62, 118.43, 116.54, 103.92; ESI-MS calculated for C<sub>15</sub>H<sub>10</sub>N<sub>2</sub>O<sub>3</sub>, [M-H]<sup>-</sup> 265.06, found 265.10.

### Synthesis of (Z)-3-(4-(4-bromobutoxy)phenyl)-2-(4-nitrophenyl)acrylonitrile (2)

(Z)-3-(4-hydroxyphenyl)-2-(4-nitrophenyl)acrylonitrile (1.06 g, 4 mmol), 1, 4-dibromo butane (1.7 ml, 20 mmol), anhydrous K<sub>2</sub>CO<sub>3</sub> (0.61 g, 4.4 mmol) and dry acetonitrile (30 ml) were added to a flask in order. The mixture was refluxed for about 6 h until one of the reactants disappeared (monitored by TLC, ethyl acetate/petroleum ether 1:1). The reaction mixture was cooled to r.t. and a resultant yellow precipitate was collected by filtering. The solid was dissolved chloroform and washed with water until the organic phase had pH 6. Upon dried over anhydrous Na<sub>2</sub>SO<sub>4</sub> and filtered, the organic phase was concentrated under reduced pressure to give a yellow solid. The crude product was recrystallized from acetonitrile to get yellow product compound **2** (1.15 g, 72%). mp 121-123 °C; IR (KBr)  $\nu$  3103, 3069, 2210, 1577, 1509, 1460, 1421, 1372, 1337, 1309 cm<sup>-1</sup>; <sup>1</sup>H NMR (400 MHz, CDCl<sub>3</sub>)  $\delta$  8.28 (d,  $J$  = 8.8 Hz, 2H), 7.94 (d,  $J$  = 8.8 Hz, 2H), 7.81 (d,  $J$  = 8.8 Hz, 2H), 7.63 (s, 1H), 6.99 (d,  $J$  = 8.8 Hz, 2H), 4.09 (t,  $J$  = 6.0 Hz, 2H), 3.50 (t,  $J$  = 6.4 Hz, 2H), 2.11 (m, 2H), 2.00 (m, 2H); <sup>13</sup>C NMR (500 MHz, DMSO-d<sub>6</sub>)  $\delta$  161.72, 147.39, 146.44,

141.06, 132.35, 126.97, 126.18, 124.75, 118.31, 115.57, 105.27, 67.51, 35.22, 29.46, 27.71; MS (MALDI-TOF): calcd. for  $C_{19}H_{17}BrN_2O_3^+$  400.04 (m/z), found 400.04.

### Synthesis of the chemosensor CDB-DMA12

To a single-necked flask, compound **2** (1.0 g, 2.5 mmol), N, N-dimethyldodecylamine (0.53 g, 2.5mmol) and acetonitrile (15mL) were added. Then, the mixture was refluxed for about 3h until one of the reactants disappeared (monitored by TLC; ethyl acetate : petroleumether = 1:1). The reaction mixture was cooled to iced temperature and a resultant yellow precipitate was collected by filtering. The residue was washed with acetone to give a yellow powder (1.3 g, 84.6%).  $^1H$  NMR (400 MHz, DMSO- $d_6$ ):  $\delta$  8.37 (d,  $J = 8.4$  Hz, 2H), 8.25 (s, 1H), 8.06 (d,  $J = 9.6$  Hz, 2H), 8.03 (d,  $J = 9.6$  Hz, 2H), 7.18 (d,  $J = 8.8$  Hz, 2H), 4.17 (t,  $J = 4.8$  Hz, 2H), 3.02 (s, 10H), 1.81 (s, 4H), 1.63 (s, 2H), 1.24 (d,  $J = 7.2$  Hz, 18H), 0.85 (t,  $J = 6.4$  Hz, 3H);  $^{13}C$  NMR (500MHz,  $d_6$ -DMSO)  $\delta$  161.60, 147.40, 146.39, 141.02, 132.37, 126.98, 126.33, 124.76, 118.29, 115.59, 105.35, 67.50, 63.30, 62.66, 50.59, 31.76, 29.52, 29.47, 29.32, 29.19, 29.01, 26.27, 25.78, 22.55, 22.14, 19.18, 14.39; MS (MALDI-TOF): calculated for  $C_{37}H_{37}N_4O_3^+$  (m/z): 534.40; found: 534.50.

### Synthesis of Model 1

To a flask,  $NaHSO_3$  (3 g, 0.0283 mol), distilled water (4.5 mL) were added. Then, benzaldehyde (3 g, 0.0283 mol) was dropped in flask slowly at room temperature. After stirring 30 minutes, the mixture was filtered. The residue was washed with saturated brine to give **Model**

**1** as a white powder (5.1g, 86%).  $^1\text{H}$  NMR (400MHz,  $\text{D}_2\text{O}$ ):  $\delta$  7.47-7.48 (2H), 7.36-7.37 (3H), 5.43 (s, 1H); ESI-MS calculated for  $\text{C}_7\text{H}_7\text{N}_a\text{O}_4\text{S}$   $[\text{M}-\text{Na}]^-$  186.99, found 187.00.

### Synthesis of Model 2

**Model 2** was synthesized according to the same synthetic method of **Model 1**. To a flask,  $\text{NaHSO}_3$  (3 g, 0.0283 mol), distilled water (4.5 mL) were added. Then, propaldehyde (1.64 g, 0.0283mol) was dropped in flask slowly at room temperature. After stirring 30 minutes, the mixture was filtered. The residue was washed with saturated brine to give **Model 2** as a white powder (12.3 g, 86%).  $^1\text{H}$  NMR (400 MHz,  $\text{D}_2\text{O}$ ):  $\delta$  4.19-4.23 (dd,  $J=3.2, 6.8$  Hz, 1H), 1.86-1.92 (m, 1H), 1.55-1.63 (m, 1H), 0.93-0.97 (t,  $J = 7.6$  Hz, 3H); ESI-MS calculated for  $\text{C}_3\text{H}_7\text{N}_a\text{O}_4\text{S}[\text{M}-\text{Na}]^-$  138.99, found 139.00.

### 2.3 UV-vis absorption and fluorescence spectrum measurements

A  $5 \times 10^{-3}$  M stock solution of **CDB-DMA12** was prepared in absolute DMSO, **SH** ( $2.5 \times 10^{-3}$  M) stock solution was prepared in double-distilled water, and the stock solutions of **Model 1**, **Model 2** and **SDS** (each at  $2.5 \times 10^{-3}$  M) were prepared in double-distilled water. In a typical detection, the test solutions of **CDB-DMA12** were firstly prepared by diluting its stock solution (35.0  $\mu\text{L}$ ) with double-distilled water to a mixed aqueous solution  $\text{H}_2\text{O}/\text{DMSO}$  (993/7, v/v) in the total volume of 5 mL, which was then added with various amount of **SH** (from 0 to 42  $\mu\text{M}$ ). Then, the solution was mixed and was transferred to a 1 cm quartz cell for absorption spectra and fluorescence spectra separately after each solution was incubated for 20 min at 25  $^\circ\text{C}$ . The comparison tests of **Model 1**, **Model 2** and **SDS** solutions were similar to that of **SH**.

All the measurements of the testing solutions were controlled and recorded at  $\text{pH}=7\pm 0.4$ . All the fluorescence spectra were recorded in the range from 470 nm to 700 nm using a 400 nm excitation wavelength. The excitation and emission bandwidths were set to 10 nm.

#### 2.4 DLS and TEM measurements

For **CDB-DMA12**, 35.0  $\mu\text{L}$  stock solution of **CDB-DMA12** were placed into a test tube and diluted to a mixed aqueous solution  $\text{H}_2\text{O}/\text{DMSO}$  (993/7) in the total volume of 5 mL with double-distilled water, which shaken gently. The average particle size of **CDB-DMA12** aggregates in solution was measured by DLS instrument after 20 min incubation at  $25^\circ\text{C}$ . For **CDB-DMA12/SH** aggregates, 35.0  $\mu\text{L}$  stock solution of **CDB-DMA12** were placed into a test tube, diluted with double-distilled water to a mixed aqueous solution  $\text{H}_2\text{O}/\text{DMSO}$  (993/7) in the total volume of 5 mL, then 70.0  $\mu\text{L}$  stock solution of **SH** were added and mixed well. The average particle size of the solution was measured by DLS instrument after incubated for 20 min at  $25^\circ\text{C}$ . The sample solution preparation for TEM measurement was similar to DLS, and each sample solution was dropped onto a carbon-coated copper grid and dried at ambient temperature, then the TEM images were observed and recorded on a JEM-2010 instrument.

#### 2.5 $^1\text{H}$ NMR titration

**CDB-DMA12** and **SH** or **SDS** were dissolved in mixed aqueous solution of  $\text{D}_2\text{O}/d_6\text{-DMSO}$  (1/3) to prepare a stock solution in a molar concentration of  $5\times 10^{-3}$  M and  $1.5\times 10^{-2}$  M,

respectively. In  $^1\text{H}$  NMR titration experiment, different amount of **SH** and **SDS** (0.5 equiv. and 1.0 equiv.) was slowly added into the **CDB-DMA12** stock solution with gently shaking, and then the mixture was incubated for 20 min at room temperature. After that, the  $^1\text{H}$  NMR spectra were measured on a Varian Gemini-400 (Bruker, 400 MHz) NMR spectrometer.

### 3. Results and discussion

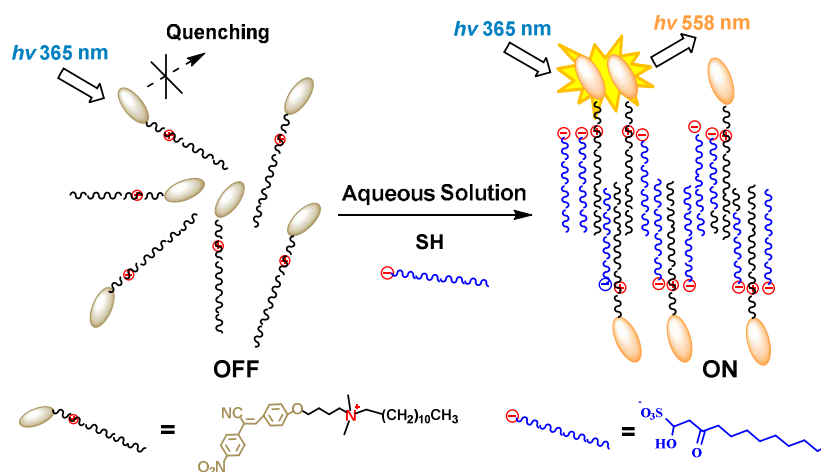
#### 3.1 Synthesis of CDB-DMA12, model 1, model 2 and the sensing strategy

The probe molecule of **CDB-DMA12** was synthesized by multi-step reaction approach (Scheme **2a**). 4-Nitrophenylacetonitrile was firstly reacted with 4-hydroxybenzaldehyde in the presence of the catalyst piperidine to prepare **1** (yield 92%), followed the coupling reaction with excessive 1,4-dibromobutane to prepare **2** (yield 72%), which was then reacted with N,N-dimethyldodecylamine to prepare **CDB-DMA12** as the probe molecule (yield 84.6%). In **CDB-DMA12**,  $\alpha$ -cyanostilbene was terminally functionalized with a quaternary ammonium unit, which offered them high solubility in aqueous solution and strong electrostatic interaction with negatively-charged molecules, besides, a 12-carbons long-aliphatic chain was attached to the quaternary ammonium moiety. The amphiphilic feature might lead to a hydrophobicity-driven arrangement in certain conditions, which could be utilized in the design of supramolecular sensors for detecting some amphiphilic molecules, especially biosurfactants and their analogs<sup>43</sup>

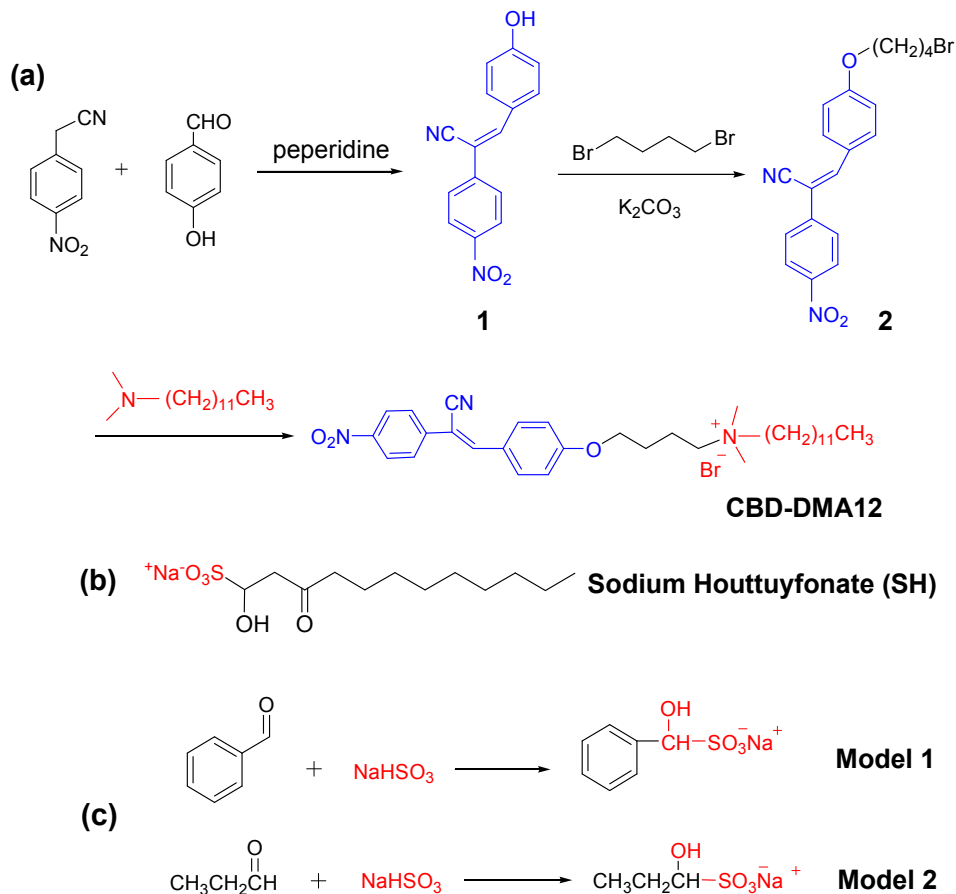
In comparison, the detection target of **SH** (Scheme **2b**), a long alkyl chain (11-carbons) amphiphilic compound bearing one sulfonyl units, was slightly soluble in water. Therefore, it

could be expected that the chemosensor **CDB-DMA12** and **SH** could interact with each other via electrostatic, hydrogen binding and hydrophobic interactions, result in the aggregation of **CDB-DMA12** and then the AIEE feature, which means the weak fluorescence emission of **CDB-DMA12** could be “turned on” after the **SH**-induced aggregation in solution. To further confirm the recognition mechanism between **CDB-DMA12** and **SH**, we also synthesized two model compounds: sodium hydroxyl(phenyl) methanesulfonate (**model 1**) and sodium 1-hydroxypropane-1-sulfonate (**model 2**) by aldehyde addition reaction, both of which lack of long alkyl chain but containing a common sulfonate units (Scheme 3c).

In sum, the detecting rationale for this AIEE based assay method is schematically depicted in Scheme 1, and the molecular characterization of the targeting products and important intermediates were shown in S3.



**Scheme 1.** Schematic illustration of the design rationale of **CDB-DMA12** for the fluorescence “turn-on” assay of **SH** via AIEE mechanism.



**Scheme 2.** (a) Synthetic pathway of **CDB-DMA12**; (b) Molecular structure of Sodium Houttuynonate (**SH**); (c) Synthetic pathway of Model **1** and **2**.

### 3.2 Fluorescence studies of **CDB-DMA12** towards **SH**

The AIE behavior of **CDB-DMA12** itself was investigated and the results were shown in S4a, b. As we know, the quaternary ammonium salt, **CDB-DMA12** is soluble in polar solvents including water, DMF, DMSO as well as other organic solvents such as methanol, acetonitrile, tetrahydrofuran and dioxane. Herein, the emission properties of **CDB-DMA12** was examined in H<sub>2</sub>O/DMSO (993/7), it showed a rather weak (almost neglectable) fluorescence emission at 520

nm in dilute aqueous solution (However, its solid showed strong fluorescence). The non-emissive feature of **CDB-DMA12** molecule in dilute solution could be attributed to its active intramolecular *cis-trans* double-bond rotation which quenched the fluorescence emission through non-radiative pathway. This much likes the non-emissive features that dissipate the energy of excitation due to the rotation of double bonds of some ammonium-containing tetraphenylethene (TPE) luminogen, which developed by Tang et al.<sup>52</sup> Whereafter, various concentrations of sodium Houttuynonate (**SH**) solution were added into the **CDB-DMA12** solution (35.0  $\mu\text{M}$ ), incubated for 20 minutes at room temperature (25 °C), and the fluorescence spectra of the **CDB-DMA12/SH** mixed solution were recorded as shown in Fig. **1a**. The fluorescence emission band was firstly red-shifted to about 558 nm and then the intensity gradually increased upon the addition of **SH** (from 0 to 42  $\mu\text{M}$ ). Accordingly, the red-shifted UV-vis absorption band of **CDB-DMA12** upon the addition of **SH** was also observed (**S4c**). On the other hand, Tang et al. recently reported a positively-charged AIEE fluorogen (TTAPE-Me) for the quantification detection of negatively-charged phospholipid Cardiolipin (CL) in inner mitochondrial membrane via electrostatic interactions.<sup>53</sup> Thus, it can be speculated and demonstrated that an AIEE (*J*-aggregation) effect was caused by **CDB-DMA12/SH**, possibly due to the positive-negative charge interactions and hydrophobic stacking between **CDB-DMA12** and **SH**.<sup>54</sup>

Based on the fluorescence “turn-on” effect, the relationship between **CDB-DMA12** fluorescence intensity (at 558 nm,  $I_{558}$ ) vs **SH** concentration was further studied (Fig. **1b**). It could be noted that the  $I_{558}$  increases linearly with the increasing of **SH** concentration in the

range of 10.5~35  $\mu\text{M}$  (0.3~1.0 equiv.,  $R^2=0.9938$ ), and then reached a platform under higher concentration of **SH** (>1.0 equiv.), suggesting **CDB-DMA12** might interact/aggregate with **SH** in 1:1 stoichiometry. According to the linear plot, the detection limit of **SH** in the present analytical approach was estimated to be 8.5  $\mu\text{M}$ . The linear relationship made **CDB-DMA12** a potential candidate for the detection of **SH** in practical application.

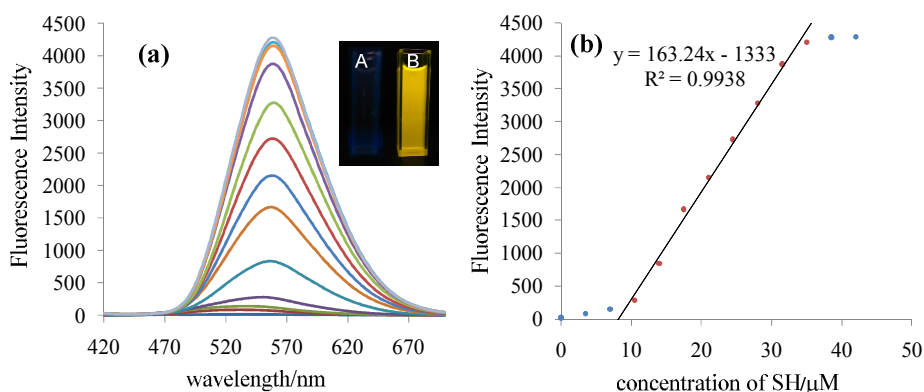


**Fig. 1** (a) Fluorescence spectra of **CDB-DMA12** (35.0  $\mu\text{M}$ ) in  $\text{H}_2\text{O}/\text{DMSO}$  (993/7, v/v) with the addition of different amount of **SH** (from 0.0 to 42  $\mu\text{M}$ ) after incubating for 20 minutes at 25  $^\circ\text{C}$ ;  $\lambda_{\text{ex}} = 400$  nm. Inset: (A) photograph of the **CDB-DMA12** solutions (35.0  $\mu\text{M}$ ) and (B) the mixed solution of **CDB-DMA12** and 1.0 equiv. of **SH** after incubating for 20 minutes at 25  $^\circ\text{C}$  under UV light (365 nm) illumination. (b) Variation of the fluorescence intensity at  $\lambda_{\text{ex}}=558$  nm against the concentration of **SH** and the linear region of the **CDB-DMA12** fluorescence intensity vs **SH** concentration.

### 3.3 Time-resolved fluorescence study of **CDB-DMA12** to **SH**

The response time<sup>55</sup> of **CDB-DMA12** to **SH** was evaluated subsequently. The fluorescence spectra of the ensemble of **CDB-DMA12** (35.0  $\mu\text{M}$ ) and **SH** (14, 21, 28, 35  $\mu\text{M}$ ) were measured after incubation for different times. As depicted in Fig. 2a, the fluorescence intensity increased gradually in the presence of 1.0 equiv. of **SH** by prolonging the reaction time from 0~30 min and

then reached a platform at room temperature (25 °C). Meanwhile, different fluorescence intensity over incubation time was also detected under the addition of various concentrations of **SH** (Fig. 2b). Notably, the response time would be shortened upon the addition of increasing amounts of **SH** (from 14 to 35  $\mu\text{M}$ ), an obvious fluorescence enhancement was detected when the added **SH** at 35  $\mu\text{M}$ . This might be explained that the presence of high concentration of **SH** could effectively accelerate the aggregation process of **CDB-DMA12** via positive-negative charges interaction, which finally resulted in the rapid enhancement of fluorescence emission.

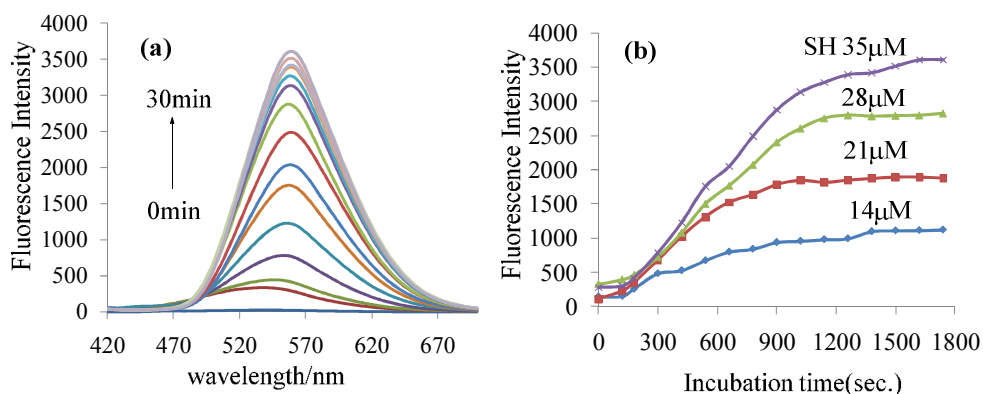


**Fig. 2** (a) Fluorescence spectra of the ensemble of **CDB-DMA12** (35.0  $\mu\text{M}$ ) and **SH** (35.0  $\mu\text{M}$ ) in  $\text{H}_2\text{O}/\text{DMSO}$  (993/7, v/v) after different incubation times at 25 °C. (b) Variation of the fluorescence intensity at 558 nm vs the incubation time for the ensemble of **CDB-DMA12** (35.0  $\mu\text{M}$ ) and various amounts of **SH** (14, 21, 28, 35  $\mu\text{M}$ ) in  $\text{H}_2\text{O}/\text{DMSO}$  (993/7, v/v),  $\lambda_{\text{ex}}=400$  nm.

### 3.4 The detecting mechanism of **CDB-DMA12** to **SH**

The controllable preparation of fluorescent micro/nanostructures with certain aggregation morphologies and functions has attracted much attention.<sup>56</sup> Considering the possible application of organic fluorescent micro/nanostructures in the fields of fluorescent labeling and/or sensing

materials, we thus measured the aggregation properties of **CDB-DMA12** amphiphile itself and **CDB-DMA12**/**SH** mixture in H<sub>2</sub>O/DMSO (993/7). It could be found that the hydrated particle size of **CDB-DMA12** (35.0 μM) was around 58.7±3.6 nm by DLS, while the particle size of the **CDB-DMA12** (35.0 μM)/**SH** (35.0 μM) aggregates was 618.7±43.6 nm (**S5**), indicating the addition of **SH** to **CDB-DMA12** would lead to the formation of large-sized supramolecular aggregation, and further caused the AIEE effect. The DLS results provide further supporting for the desired mechanism of AIEE “turn-on” assay for **SH** (see Scheme 1). Moreover, the morphology of **CDB-DMA12** and **CDB-DMA12**/**SH** aggregation were observed by TEM as shown in Fig. **3a, b**. It could be seen that **CDB-DMA12** (35.0 μM) formed 50-120 nm granule-shaped nanoparticles, interestingly, **CDB-DMA12** (35.0 μM) /**SH** (35.0 μM) aggregation formed sheet, scroll and tube-shaped nanoaggregates with the length of 0.5-1.5 μm and width of 100-200 nm (Fig. **3c, d**). The morphology change from nanoparticles to sheet, scroll and tube-shaped nanoaggregates suggested clearly that **CDB-DMA12** were arranged orderly in the presence of **SH**, which might primarily be driven by electrostatic interaction, hydrogen binding and hydrophobic stacking of the long chain or active group sites. So, it could be expected that certain morphology of fluorescent nano-aggregate could be obtained by direct mixing various of oppositely-charged small molecular amphiphiles in aqueous solution, which offered a simple but efficient self-assembly approach for the preparation of micro/nano-scaled fluorescent materials and devices.

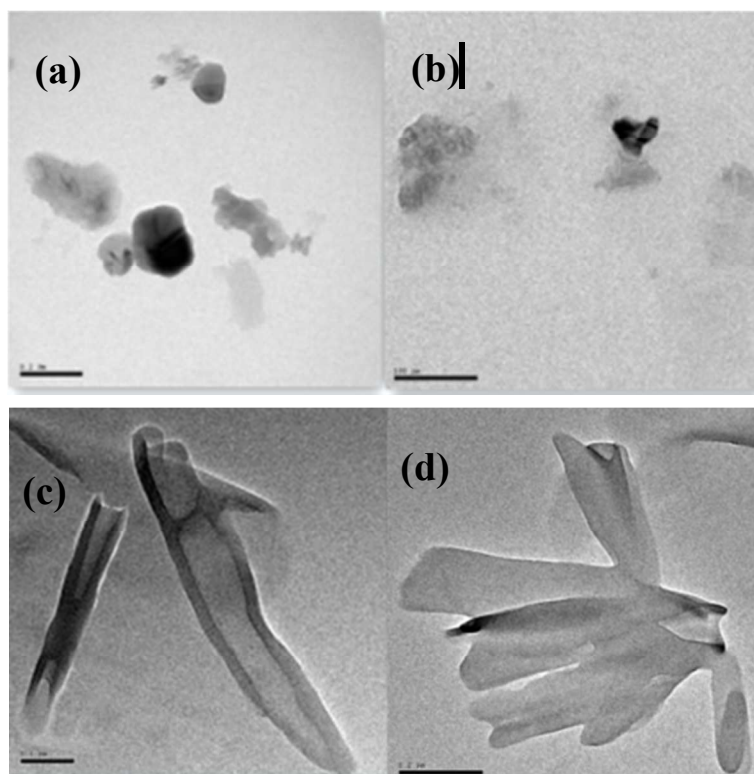


**Fig. 3** TEM images for **CDB-DMA12** ( $35.0 \mu\text{M}$ ) in the absence of **SH** ( $35.0 \mu\text{M}$ ) (a) bar  $0.2 \mu\text{m}$ ; (b) bar  $100 \text{ nm}$  and in the presence of **SH** ( $35.0 \mu\text{M}$ ) (c) bar  $0.2 \mu\text{m}$ ; (d) bar  $0.2 \mu\text{m}$ .

In order to further investigate the molecular recognition and the following self-assembly processes between **CDB-DMA12** and **SH**,  $^1\text{H}$  NMR titration experiment was conducted with the addition of **SH** into **CDB-DMA12** (S6a). It could be seen that the protons on the **CDB-DMA12** displayed an upfield shifts with the addition of **SH**, which indicated that the formation of **CDB-12DMA/SH** complexes were introduced via the electrostatic forces of opposite charges, the hydrophobic interactions between the long alkyl chains and the hydrogen bindings of the active group sites (such as hydroxyl and carbonyl in **SH**, cyano-group and ether oxygen unit in **CDB-DMA12**). Furthermore, the  $^1\text{H}$  NMR titration of **CDB-DMA12** with the addition of **SDS** was

also evaluated. It could be seen that the protons shifts on the **CDB-DMA12** almost have no changes, which indicate that there are no form of **CDB-DMA12/SDS** complexes via electrostatic forces of opposite charges, or any hydrogen bindings and hydrophobic interactions (**S6b**). The possible pattern and acting sites between **CDB-DMA12 /SH** was shown in **S6a**.

All these experimental facts caused us to speculate the molecular recognition and self-assembly process of **CDB-DMA12/SH**. It could be seen that the quaternary ammonium group in **CDB-DMA12** tends to attract with the sulfonyl group in **SH**, due to the strong electrostatic interaction between the opposite charges and the hydrogen binding interaction of the active group sites. Meanwhile, long alkyl chains both of **CDB-DMA12** and **SH** orderly arranged along with each other via hydrophobic stacking interaction, and the hydrophobic  $\alpha$ -cyanostilbene units of **CDB-DMA12** were twisted towards the long alkyl chains region. Simultaneously, the planar  $\alpha$ -cyanostilbene units would stack onto each other “side by side” (denoted as *J*-aggregation, which brings red-shift in absorption and emission spectra) via  $\pi$ - $\pi$  interactions and formed relatively “rigid” architectures, which resulted in the diminish of non-emissive decay of **CDB-DMA12** and lead to the AIEE effect.<sup>30</sup> Afterward, more and more of **CDB-DMA12** and **SH** amphiphiles attached and orderly arranged onto the pre-organized **CDB-DMA12/SH** assemblies/templates and finally caused the formation of sheet, scroll and tube-shaped aggregates.

### 3.5 Selectivity of **CDB-DMA12** for **SH**

Based on the above-mentioned results, it could be noted that the long hydrophobic chains might play essential roles in the recognition of **CDB-DMA12** for **SH** via AIEE mechanism. Thus, in order to confirm the effect of hydrophobic chain to **SH** sensing and to further examine the selectivity of **CDB-DMA12** to **SH** among the negative-charged organosulfonates, two model compounds **Model 1** (hydroxy-aryl-methanesulfonate) and **Model 2** (hydroxy-aliphatic-methanesulfonate), both of which lacking long alkyl chain but containing sulfonyl group species, one represent aryl-methanesulfonate and the other stand for aliphatic-methanesulfonate, were synthesized and employed for comparison. Furthermore, sodium dodecyl sulfonate (**SDS**), sodium dodecyl benzene sulfonate (**SDBS**), sodium hexadecyl sulphate (**AS**), common-used anion surfactant, were also used as references, since which have similar long alkyl chain structure to **SH**. As shown in Fig. **4a**, the addition of **Model 1** and **Model 2** (0-1.2equiv), **SDBS** and **AS** (0-1.2equiv) to **CDB-DMA12** (35.0  $\mu\text{M}$ ) did not lead to obvious fluorescence enhancement (1.0-1.1fold) at 558 nm, although they possessed hydroxy-sulfonyl groups or mono-sulfonyl groups like **SH**. On the other hand, the fluorescent intensity of **CDB-DMA12** increased upon the addition of **SDS** (the **SDS** concentration was 0-0.8 equiv.), and reached a peak (about 15-fold enhancement) at about 0.8 equiv., then drastically decreased to its original when added high concentration of **SDS** (0.8-1.2 equiv.). This is possibly due to the competition binding of **SDS** to **CDB-DMA12**, which only have electrostatic and hydrophobic driven effects to induce the aggregation of **CDB-DMA12**, but lack the relevant active sites of the hydrogen bonding interactions and could not be achieved a stability. Therefore, excessive **SDS** (0.8-1.2

equiv.) would disrupted the pre-organized **CDB-DMA12/SDS** assembly. These could also be illustrated by the  $^1\text{H}$  NMR titration experiment of **SDS** to **CDB-DMA12** (**S6b**), of which changes in the shifts with the addition of **SDS** (0.5 equiv.), but recovers upon the addition of **SDS** (1.0 equiv.). In contrast, the fluorescence of **CDB-DMA12** significantly enhanced with the addition of **SH** (0-1.2 equiv.), and then reached a platform (52-fold) at around 1.0 equiv., much higher than that of **SDS** (1.7-fold), **Model 1** (1.1-fold) and **Model 2** (1.1-fold) at the same molar concentration (Fig. **4b**). Notably, the fluorescence emission still maintained under excessive **SH**, elicited that **CDB-DMA12** could efficiently bind with **SH** to form stable aggregates, and which would not be dissociated upon the adding of oppositely-charged species/analytes. These results clearly indicated that **CDB-DMA12** shows good selectivity toward **SH** among the negative-charged organosulfonates, which might due to the synergistic recognition effect between **CDB-DMA12** and **SH** by combining the hydrophobic stacking of the long alkyl chains, the electrostatic interaction of the opposite charges and the hydrogen binding of the active group sites. The color-change from light yellow to dark yellow upon the addition of **SH** to **CDB-DMA12** could even be observed by naked-eyes, whereas upon the addition of **SDS**, **Model 1** and **Model 2** induced different color-change from light yellow to colorless (Fig. **5**). All of these indicated that **CDB-DMA12** has high selectivity to **SH** among the analytes. So, it demonstrated that **CDB-DMA12** could be possibly employed in the practical detection of **SH** among the sulfonyl-containing molecular species. In addition, the structure-recognition relationship study of the quaternary ammonium salts of  $\alpha$ -cyanostilbene derivatives **CDB1-5** and **CDB-DMA12**

would be benefit for the rational design of AIEE-based sensors via selective supramolecular assembly.

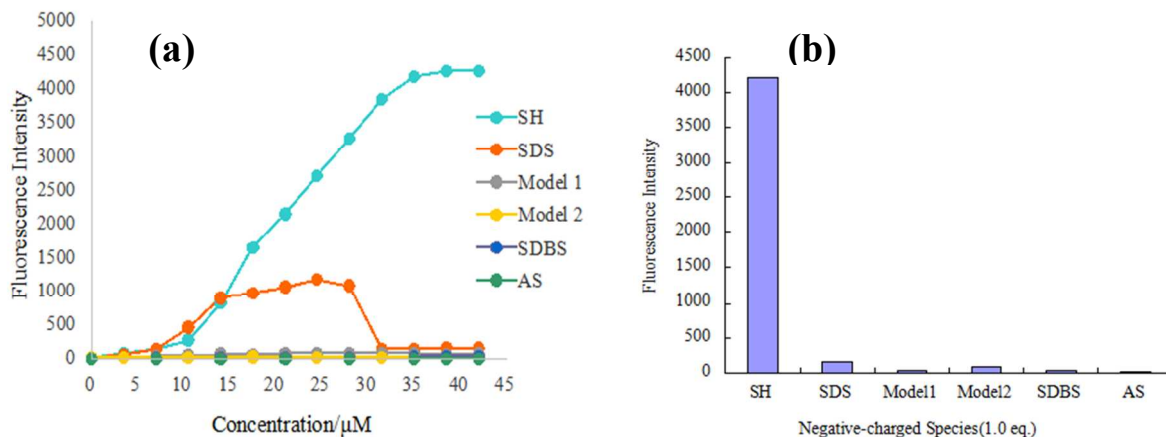


**Fig. 4** (a) Variation of the fluorescence intensity of **CDB-DMA12** (35.0  $\mu\text{M}$ ) in  $\text{H}_2\text{O}/\text{DMSO}$  (993/7, v/v) upon addition of different concentrations of **SH**, **SDS**, **Model 1**, **Model 2**, **SDBS** and **AS** (from 0.0 to 42.0  $\mu\text{M}$ ) respectively ( $\lambda_{\text{ex}} = 400 \text{ nm}$ ); (b) the fluorescence intensity (at 558 nm) after the addition of **SDBS**, **AS**, **Model 1**, **Model 2**, **SDS** and **SH** (1.0 equiv.); each solution was incubated for 20.0 min before fluorescence measurements.

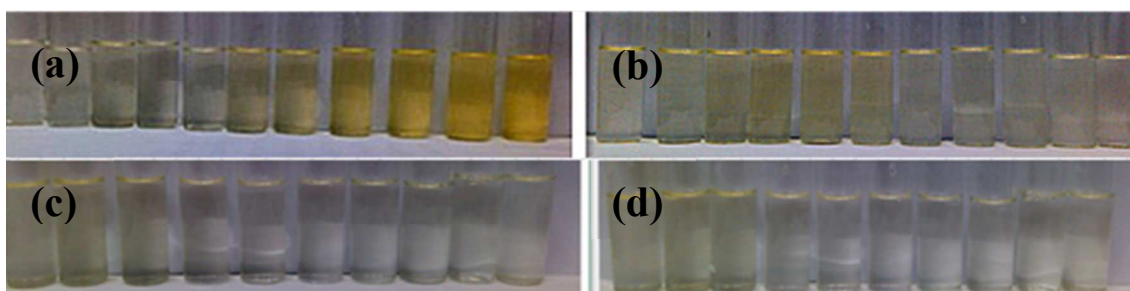


**Fig. 5** Visual color changes of the solutions of **CDB-12DMA** (35.0  $\mu\text{M}$ ) in  $\text{H}_2\text{O}/\text{DMSO}$  (993/7, v/v) with the addition of 0, 0.1, 0.2, 0.3, 0.4, 0.5, 0.6, 0.7, 0.8, 0.9, 1.0 equiv. (from left to right) of (a) **SH**, (b) **SDS**; and 0, 0.1, 0.2, 0.3, 0.4, 0.5, 0.6, 0.7, 0.8, 0.9 equiv. (from left to right) of (c) **Model 1**, (d) **Model 2**

## 4. Conclusions

In summary, we have successfully developed a new fluorescence ‘turn-on’ assay method for Sodium Houttuynonate (**SH**), the designation of this sensing system is based on the synergistic effect of the electrostatic interaction between the quaternary ammonium and sulfonyl groups, the hydrogen binding of the active group sites, as well as the hydrophobic stacking between the long alkyl chains in  $\alpha$ -cyanostilbene derivative **CDB-DMA12** and Sodium Houttuynonate (**SH**). The recognition between  $\alpha$ -cyanostilbene derivative **CDB-DMA12** and Sodium Houttuynonate (**SH**) could induce obvious fluorescence enhancement and visible absorption red-shifting (by naked eyes). Accordingly, a linear relationship was found when plot the fluorescence intensity at 558 nm and Sodium Houttuynonate (**SH**) concentration, with an estimated detection limit of 8.5  $\mu\text{M}$ . Furthermore, morphology changes from nanoparticles to sheet, scroll and tube-shaped aggregates were observed. Notably,  $\alpha$ -cyanostilbene derivative **CDB-DMA12** showed high selectivity to Sodium Houttuynonate (**SH**) among other sulfonyl containing species, attributed to the synergistic effect of its quaternary ammonium, the hydrogen binding of the active group sites and a twelve carbon containing long-aliphatic chain units. In addition, the current work paved a new way for detection/recognition of amphiphilic natural products in aqueous solution. Besides, it also provided a possible approach for preparation of fluorescent micro/nano-scaled architectures through the solution self-assembly of oppositely-charged small organic amphiphiles.

## ASSOCIATED CONTENT

### Supporting Information

Characterization of intermediates and probe; UV-vis absorption spectra and  $^1\text{H}$  NMR titration of **CDB-DMA12** with the addition of different amount of **SH** and the dynamic light scattering results. This material is available free of charge via the Internet at <http://www.rsc.org/>.

### Acknowledgements

We thank the Science and Technology Innovation Foundation for the College Students of Beijing (No. 13220055), the National Science Foundation of China (No. 21575012 and 21372251), and the Natural Science Foundation of Beijing (No. 2151003) for financial support. We also thank the inspirer and the discussing of Professor **Dihua Shangguan** in Key Laboratory of Analytical Chemistry for Living Biosystems, Institute of Chemistry, CAS.

### Notes and references

- 1 T. Kosuge, *J. Pharm. Soc. Jpn.*, 1952, **72**, 12271-12275.
- 2 P. Pan, Y. J. Wang, L. Han, X. Liu, M. Zhao, Y. F. Yuan, *J. Ethnopharmacol.*, 2010, **131**, 203-209.
- 3 J. Shao, H. Cheng, D. Wu, C. Wang, L. Zhu, Z. Sun, Q. Duan, W. Huang, J. Huang, *J. Tradit. Chin. Med.*, 2013, **33** (6), 798-803.
- 4 X. Ye, X. Li, L. Yuan, L. Ge, B. Zhang, S. Zhou, *Colloids Surf. A*, 2007, **301**, 412-418.
- 5 X. Ye, L. Xu, X. Li, Z. Chen, B. Zhang, L. Yuan, X. Chen, H. Zhang, W. Chang, S. Sun, *Colloids Surf. A*, 2009, **350**, 130-135.
- 6 D. Wang, Q. Yu, P. Eikstadt, D. Hammond, Y. Feng, N. Chen, *Int. Immunopharmacol.*, 2002, **2**, 1411-1418.
- 7 X. L. Ye, X. G. Li, L. J. Yuan, *Colloids Surf. A*, 2005, **268**, 85-89.
- 8 X. L. Ye, X. G. Li, L. J. Yuan, *J. Asian Nat. Prod. Res.*, 2006, **8**, 327-334.
- 9 L. J. Yuan, X. G. Li, H. M. He, *Chinese J. Trad. Med.*, 2005, **20**, 268-271.
- 10 Z. Deng, D. Zhong, X. Chen, *Biomed. Chromatogr.*, 2012, **26** (11), 1377-1385.

- 11 X. Duan, D. Zhong, X. Chen, *J. Mass Spectrom.*, 2008, **43** (6), 814-824.
- 12 K. P. Carter, A. M. Young, A. E. Palmer, *Chem. Rev.*, 2014, **114** (8), 4564-4601.
- 13 D. Z. Li, Y. X. Yang, C. Yang, B.W. Hu, B. L. Huo, L.W. Xue, A. Z. Wang, F. F. Yu, *Tetrahedron*, 2014, **70**, 1223-1229.
- 14 R. N. Dsouza, U. Pischel, W. M. Nau, *Chem. Rev.*, 2011, **111** (12), 7941-7980.
- 15 M. Vendrell, D. Zhai, J. C. Er, Y. T. Chang, *Chem. Rev.*, 2012, **112** (8), 4391-4420.
- 16 X. Zhang, J. Yin, J. Yoon, *Chem. Rev.*, 2014, **114** (9), 4918-4959.
- 17 J.-H. Ye, L. J. Duan, C. C. Yan, W. C. Zhang, W. J. He, *Tetrahedron Lett.*, 2012, **53**, 593-596.
- 18 J. Luo, Z. Xie, W. Y. Lam, *Chem. Commun.*, 2001, **11**: 1740- 1741.
- 19 B. Z. Tang, X. W. Zhan, G. Yu, P. P. S. Lee, Y. Liu, D. Zhu *J. Mater. Chem.*, 2001, **11**, 2974-2978.
- 20 Y. N. Hong, J. W. Y. Lam, B. Z. Tang, *Chem. Commun.*, 2009, 4332-4353.
- 21 X. Q. Zhang, X. Y. Zhang, L. Tao, Z. G. Chi, J. R. Xu, Y. Wei, *J. Mater. Chem. B*, 2014, **2**, 4398-4414.
- 22 G. S. Zhao, C. X. Shi, Z. Q. Guo, W. H. Zhu, S. Q. Zhu, *Chin. J. Org. Chem.*, 2012, **32**, 1620 ~1632.
- 23 X. Q. Zhang, X. Y. Zhang, S. Q. Wang, M. Y. Liu, L. Tao, Y. Wei, *Nanoscale*, 2013, **5**, 147-150.
- 24 X. Q. Zhang, Z. G. Chi, Y. Zhang, S. W. Liu, J. R. Xu, *J. Mater. Chem. C*, 2013, **1**, 3376-3390.
- 25 B. Vandana, K. Sharanjeet, V. Varun, K. Manoj, *Inorg. Chem.*, 2013, **52**, 4860-4865.
- 26 C. W. T. Leung, Y. N. Hong, S. J. Chen, E. G. Zhao, J. W. Y. Lam, B. Z. Tang, *J. Am. Chem. Soc.*, 2013, **135**, 62-65.
- 27 S. Song, Y. S. Zheng, *Org. Lett.*, 2013, **15**(4), 820-823.
- 28 Y. Liu, C. M. Deng, L. Tang, A. J. Qin, R. R. Hu, J. Z. Sun, B. Z. Tang, *J. Am. Chem. Soc.*, 2011, **133**, 660-663.
- 29 P. C. Xue, R. Lu, P. Zhang, J. H. Jia, Q. X. Xu, T. R. Zhang, M. Takafuji, H. Ihara, *Langmuir*, 2013, **29**, 417-425.
- 30 L. K. Wang, Y. F. Shen, Q. J. Zhu, W. N. Xu, M. D. Yang, H. P. Zhou, J. Y. Wu, Y. P. Tian, *J. Phys. Chem. C*, 2014, **118**, 8531-8540.
- 31 C. Q. Zhang, S. B. Jin, S. L. Li, X. D. Xue, J. Liu, Y. R. Huang, Y. G. Jiang, W. Q. Chen, G. Z. Zou, X. J. Liang, *ACS Appl. Mater. Interfaces*, 2014, **6**, 5212-5220.
- 32 Y. N. Jiang, X. D. Yang, C. Ma, C. X. Wang, Y. Chen, F. X. Dong, B. Yang, K. Yu, Q. Lin, *ACS Appl. Mater. Interfaces*, 2014, **6**, 4650-4657.
- 33 D. Ding, K. Li, B. Liu, B. Z. Tang, *Accounts Chem. Res.*, 2013, **46** (11), pp 2441-2453.
- 34 A. Z. Wang, Y. X. Yang, F. F. Yu, L.W. Xue, B. W. Hu, Y. J. Dong, W. P. Fan, *Anal. Methods*, 2015, **7**, 2839 - 2847.
- 35 J. Mei, Y. Hong, J. W. Y. Lam, A. J. Qin, Y. H. Tang, B. Z. Tang, *Adv. Mater.*, 2014, **26**, 5429-5479.

- 36 Y. S. Zheng, Y. J. Hu, *J. Org. Chem.*, 2009, **74**, 5660–5663.
- 37 Y. S. Zheng, Y. J. Hu, D. M. Li, Y. C. Chen, *Talanta*, 2010, **80**, 1470–1474.
- 38 D. M. Li, Y. S. Zheng, *Chem. Commun.*, 2011, **47**, 10139–10141.
- 39 D. M. Li, Y. S. Zheng, *J. Org. Chem.*, 2011, **76**, 1100–1108.
- 40 B. K. An, J. Gierschner, S. Y. Park, *Accounts Chem. Res.*, 2012, **45**, 544–554.
- 41 L. L. Zhu, Y. L. Zhao, *J. Mater. Chem. C*, 2013, **1**, 1059–1065.
- 42 A. Z. Wang, Y. X. Yang, F. F. Yu, L. W. Xue, B. W. Hu, W. P. Fan, Y. J. Dong, *Talanta*, 2015, **132**: 864–870.
- 43 L. T. Zeng, J. S. Wu, Q. Dai, W. M. Liu, P. F. Wang, C. S. Lee, *Org. Lett.*, 2010, **12**, 4014–4017.
- 44 M. H. Lan, W. M. Liu, Y. Wang, J. C. Ge, J. S. Wu, H. Y. Zhang, J. H. Chen, W. J. Zhang, P. F. Wang, *ACS Appl. Mater. Interfaces*, 2013, **5**, 2283–2288.
- 45 L. T. Zeng, P. F. Wang, H. Y. Zhang, X. Q. Zhuang, Q. Dai, W. M. Liu, *Org. Lett.*, 2009, **11**, 4294–4297.
- 46 X. Shen, G. X. Zhang, D. Q. Zhang, *Org. Lett.*, 2012, **14**, 1744–1747.
- 47 M. Wang, X. G. Gu, G. X. Zhang, D. Q. Zhang, D. B. Zhu, *Anal. Chem.*, 2009, **81**, 4444–4449.
- 48 Q. Dai, W. M. Liu, X. Q. Zhuang, J. S. Wu, H. Y. Zhang, P. F. Wang, *Anal. Chem.*, 2011, **83**, 6559–6564.
- 49 X. Q. Chen, S. Kang, M. J. Kim, J. Kim, Y. S. Kim, H. Kim, B. Chi, Sung-Jin Kim, J. Y. Lee, J. Yoon, *Angew. Chem., Int. Ed.*, 2010, **49**, 1422–1425.
- 50 E. Climent, C. Giménez, M. D. Marcos, R. Martínez-Mañez, F. Sancenón, J. Soto, *Chem. Commun.*, 2011, **47**, 6873–6875.
- 51 S. Kumar, S. Arora, P. Singh, S. Kumar, *RSC Adv.*, 2012, **2**, 9969–9975.
- 52 W. Z. Yuan, H. Zhao, X. Y. Shen, F. Mahtab, J. W. Y. Lam, J. Z. Sun, B. Z. Tang, *Macromol.* 2009, **42**, 9400–9411.
- 53 C. W. T. Leung, Y. Hong, J. Hanske, E. Zhao, S. Chen, E. V. Pletneva, B. Z. Tang, *Anal. Chem.* 2013, **86**, 1263–1268.
- 54 T. D. Slavnova, H. Görner, A. K. Chibisov, *J. Phys. Chem. B*, 2007, **111**, 10023–10031.
- 55 M. Kumar, V. Viji, V. Bhalla, *Langmuir*, 2012, **28**, 12417–12421.
- 56 B. K. An, S. H. Gihm, J. W. Chung, C. R. Park, S. K. Kwon, S. Y. Park, *J. Am. Chem. Soc.*, 2009, **131**, 3950–3957.

**Graphics of the contents**

A  $\alpha$ -cyanostilbene derivative was synthesized for the selective detection of Sodium Houttuynonate via AIEE in obvious fluorescence enhancement and a linear relationship.

